



## THE NON-AXISYMMETRIC POSTBUCKLING BEHAVIOUR OF SHALLOW SPHERICAL DOMES†

E. I. GRIGOLYUK and Ye. A. LOPANITSYN

Moscow

e-mail: eal@mami.ru

(Received 3 March 2003)

The non-axisymmetric postbuckling behaviour of an elastic, shallow spherical dome, which is rigidly clamped along its contour and loaded with a uniform transverse pressure, is considered. The solution of the problem is constructed using the Rayleigh–Ritz method based on the Marguerre equations in which the displacements in the circumferential direction are approximated by a Fourier series, and the radial displacements by Bessel functions. The resulting system of non-linear algebraic equations is solved by prolongation methods. It is shown for the first time that a shell has postbuckling, non-axisymmetric equilibrium states with loads which are significantly less than the upper critical load as well as the loads corresponding to bifurcation points. It is suggested that, taking into account the forms of these equilibrium states as the initial inaccuracies of a spherical dome should enable one to model the spread in its experimentally obtained critical loads. © 2004 Elsevier Ltd. All rights reserved.

The principal aim of the solution of the problem of the postbuckling behaviour of shells is to determine their equilibrium states under conditions when the shell has already lost its load-bearing capacity. These equilibrium states are unstable and cannot be realized under operational conditions. However, a knowledge of the complete pattern of the behaviour of a shell enables one to look at the process of its deformation in another way and to understand those phenomena, which remain unexplained from the points of view of idealized mathematical models of a shell. The problem of the disagreement between the theoretical and experimental data on critical loads in the case of thin-walled and, in particular, shallow spherical domes as the objects which are studied in the greatest detail in this project can serve as an example of this.

The history of this problem covers a period of almost 100 years. The paper by Bach [1] in 1902 is apparently the first experimental investigation in which it was discovered that a spherical shell turns out to be unstable at a certain external pressure. Thirteen years later, in 1915, the first paper concerned with calculating the stability of thin, elastic, spherical shells came to light. This is the dissertation by Zölly [2]. In this dissertation, a formula for the lowest critical pressure  $q = 2E[3(1 - \nu^2)]^{1/2}(h/R)^2$ , where  $E$  is the Young's modulus of the shell material,  $\nu$  is its Poisson's ratio,  $h$  is the wall thickness of the shell and  $R$  is its radius, was obtained in a linear formulation. In 1922, an attempt was made by Schwerin [3] to refine Zölly's approximate formula by an exact analytical solution of the linear, axisymmetric equations for a shallow spherical shell. However, it turned out that Zölly's formula was confirmed: calculations using it and also Schwerin's formulae only gave a difference in the third decimal place in the values for the lowest critical load. Much later, in 1939, Boley and Sechler (see [4]) carried out a careful experiment with a copper hemisphere and established that the critical pressure is a quarter of the theoretical value given by Zölly's formula.

The subsequent development of research in this field is characterized, on the one hand, by a constant increase in the experimentally obtained data on the values of the critical loads for various spherical shells and, on the other hand, by endless attempts to provide them with a theoretical basis. For this purpose, calculations have been carried out, using linear theory, account has been taken of the instantaneous stress–strain state of a shell before loss of stability, the geometrically non-linear equations of the theory of shells have been used and shells with initial imperfections in their form, contour conditions and methods of loading, and shells with the possibility of elastoplastic deformation of the material, etc. have been considered. A detailed discussion of this development of the theory and practice of the analysis of spherical shells can be found in [5–7], as well as in the reviews [8–10] and the monograph [11].

A comparison of the experimental and theoretical values of the critical loads for the loss of stability of a thin, shallow spherical shell of constant thickness acted upon by a uniform transverse pressure is

†Prikl. Mat. Mekh. Vol. 67, No. 6, pp. 921–932, 2003.

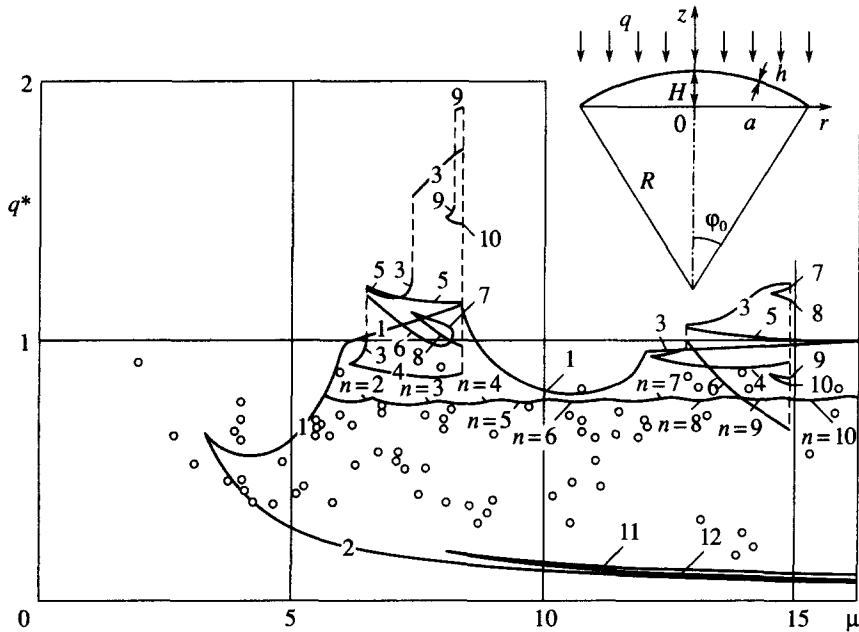


Fig. 1

shown in Fig. 1. Here,  $q^* = [3(1 - \nu^2)]^{1/2} qR^2 / (2Eh^2)$  is the dimensionless transverse pressure and  $\mu = [12(1 - \nu^2)]^{1/4} [a^2 / (Rh)]^{1/2}$  is the wall-thickness parameter of the shell. The theoretical dependences of the upper critical load  $q^*_+$  and lower critical load  $q^*_-$  of an axisymmetrically deformed spherical dome on its wall-thickness parameter are shown by the solid lines with the numbers 1 and 2. They were obtained by different researchers by solving the Marguerre and Reissner equations. Values for the upper critical load, taken from the experimental papers of different investigators (see [11]), are shown by the points.

Attempts to refine the values of the upper critical load of a shallow spherical dome by considering its axisymmetric postbuckling behaviour are represented by the papers [12–14]. Some results from [14] are labelled with the numbers 3 to 12 in Fig. 1.

It can be seen that the introduction into the calculation of a small initial inaccuracy, which is proportional to the deflection of the dome and characteristic of curves 4 and 6, enables one to reduce its upper critical load. However, this reduction stays within the limits of tens of percent.

Investigations [15, 16] dating from 1960 are the first in which the finite non-axisymmetric buckling of a shallow spherical dome, rigidly clamped along its contour and acted upon by a uniform pressure, was considered. Over a period of two years after this, the papers [17–19], in which the results of a calculation of the non-axisymmetric critical loads for the same dome were given, came to light. However, the reliability of these results gave rise to doubt. It was only in 1963 that reliable values of non-axisymmetric critical loads were successfully obtained [20] although, here also, the author proved to be liable to error. It was shown in [21] that, due to the simplified description of the radial and circumferential forces, he obtained a low asymptotic estimate of the least critical pressure in the case of a thin shell with a large number of waves along the circumference. However, this error had no effect on the main results, which were obtained numerically. A curve showing the magnitude of the lowest non-axisymmetric critical load according to [20] is denoted by the values  $n = 2, 3, \dots, 10$  in Fig. 1, where  $n$  is the number of waves along the circumference of the dome which corresponds to this load.

An acceptable compromise between the calculated and experimental data was found by a group of Japanese researchers who, in formulating the experiments in [22, 23], measured the initial deflection of each unloaded shell, which appears after it has been clamped to the laboratory stand and is a random, non-axisymmetric function of the coordinates of the points of the shell surface, in addition to the deflection of the shell and the loads corresponding to it. These data on the initial deflection of the shell were used to calculate the initially non-axisymmetric deformation of the shell with its snapping and subsequent complete turning inside out [24, 25]. A high degree of agreement between the theoretical and experimental values of the upper critical load was obtained as a result.

In view of what has been said above, the purpose of this paper is to solve the complete problem of the geometrically non-linear deformation of a shallow spherical dome, taking into account the possibility

of its non-axisymmetric loss of stability and its non-axisymmetric postbuckling behaviour and to find those forms of initial inaccuracy using, which it should be possible to obtain, the whole spectrum of experimentally obtained critical loads.

1. MATHEMATICAL MODEL OF A DOME

Among the existing methods of representing the non-axisymmetric deformations of a shallow spherical dome with finite deflection, which is treated in the polar system of coordinates  $r$  and  $\theta$ , the simplest, tested and sufficiently accurate method is the method, based on a quadratic law to describe the deformations

$$\begin{aligned}
 e_{rr} &= \frac{\partial u}{\partial r} - \frac{w}{R} + \frac{\vartheta_r^2}{2}, & \kappa_{rr} &= -\frac{\partial^2 w}{\partial r^2} \\
 e_{r\theta} &= \frac{\partial v}{\partial r} - \frac{v}{r} + \frac{1}{r} \frac{\partial u}{\partial \theta} + \vartheta_r \vartheta_\theta, & \kappa_{r\theta} &= -\frac{1}{r} \left( \frac{\partial^2 w}{\partial r \partial \theta} - \frac{1}{r} \frac{\partial w}{\partial \theta} \right) \\
 e_{\theta\theta} &= \frac{1}{r} \frac{\partial v}{\partial \theta} + \frac{u}{r} - \frac{w}{r} + \frac{\vartheta_\theta^2}{2}, & \kappa_{\theta\theta} &= -\frac{1}{r} \left( \frac{1}{r} \frac{\partial^2 w}{\partial \theta^2} + \frac{\partial w}{\partial r} \right)
 \end{aligned}$$

where  $e_{rr}, e_{r\theta}, e_{\theta\theta}, \kappa_{rr}, \kappa_{r\theta}$  and  $\kappa_{\theta\theta}$  are the deformations and curvatures of the middle surface of the dome,  $u$  and  $v$  are the radial and circumferential displacements of the points of the middle plane of the dome,  $w$  is the deflection and  $\vartheta_r = -\partial w / \partial r$  and  $\vartheta_\theta = -\partial w / (r \partial \theta)$  are the angles of rotation of the normal to the middle surface of the dome in the radial and circumferential directions.

Using Hooke's law, these deformation relations give the following expressions for the potential deformation of a dome and the work of the transverse pressure applied to it

$$\begin{aligned}
 \Pi &= \frac{1}{2} \int_0^{a/2\pi} \int_0^a \left\{ B \left[ e_{rr}^2 + 2\nu e_{rr} e_{\theta\theta} + \frac{1-\nu}{2} e_{r\theta}^2 + e_{\theta\theta}^2 \right] + \right. \\
 &\quad \left. + D \left[ \kappa_{rr}^2 + 2\nu \kappa_{rr} \kappa_{\theta\theta} + (1-\nu) \kappa_{r\theta}^2 + \kappa_{\theta\theta}^2 \right] \right\} r dr d\theta
 \end{aligned} \tag{1.1}$$

$$A = \int_0^{a/2\pi} \int_0^a q w r dr d\theta \tag{1.2}$$

Here,  $D = Eh^3/[12(1-\nu^2)]$  is the cylindrical stiffness of the dome wall and  $B = Eh/(1-\nu^2)$  is its stiffness to stretching and compression.

The potential energy of the deformation of the dome and the work of the transverse pressure applied to it enable us to obtain from the Lagrange variational equation

$$\delta(\Pi - A) = 0 \tag{1.3}$$

the Marguerre equilibrium equations

$$\begin{aligned}
 \nabla^2 \nabla^2 F + \frac{Eh}{R} \nabla^2 w + \frac{Eh}{2} N_2(w, w) &= 0 \\
 D \nabla^2 \nabla^2 w - \frac{1}{R} \nabla^2 F - N_2(F, w) &= -q; \quad 0 \leq r \leq a, \quad 0 \leq \theta \leq 2\pi
 \end{aligned} \tag{1.4}$$

and the corresponding boundary conditions for the case of rigid clamping along the contour

$$\begin{aligned}
 u, v, w, \vartheta_r, N_{rr}, \dots, Q_r^0 &\text{ are bounded functions when } r = 0 \\
 u = v = w = \vartheta_r &= 0 \text{ when } r = a
 \end{aligned} \tag{1.5}$$

where  $\nabla^2$  is the Laplace operator and  $N_2$  is the second order non-linear differential operator

$$\nabla^2 = \frac{\partial^2}{\partial r^2} + \frac{1}{r} \frac{\partial}{\partial r} + \frac{1}{r^2} \frac{\partial^2}{\partial \theta^2}$$

$$N_2(\xi, \zeta) = \frac{1}{r} \frac{\partial^2 \zeta}{\partial r^2} \left( \frac{\partial \xi}{\partial r} + \frac{1}{r} \frac{\partial^2 \xi}{\partial \theta^2} \right) - 2 \frac{\partial}{\partial r} \left( \frac{1}{r} \frac{\partial \xi}{\partial \theta} \right) \frac{\partial}{\partial r} \left( \frac{1}{r} \frac{\partial \zeta}{\partial \theta} \right) + \frac{1}{r} \frac{\partial^2 \xi}{\partial r^2} \left( \frac{\partial \zeta}{\partial r} + \frac{1}{r} \frac{\partial^2 \zeta}{\partial \theta^2} \right)$$

$F$  is the Airy force function, which is associated with the specific normal and specific shear forces by the following relations

$$N_{rr} = \frac{1}{r} \left( \frac{\partial F}{\partial r} + \frac{1}{r} \frac{\partial^2 F}{\partial \theta^2} \right), \quad N_{r\theta} = \frac{1}{r} \left( \frac{1}{r} \frac{\partial F}{\partial \theta} - \frac{\partial^2 F}{\partial r \partial \theta} \right), \quad N_{\theta\theta} = \frac{\partial^2 F}{\partial r^2}$$

and  $Q_r^0$  is the generalized radial specific transverse force

$$Q_r^0 = -D \frac{\partial}{\partial r} \left[ \nabla^2 w + (1 - \nu) \frac{\partial}{\partial r} \left( \frac{1}{r} \frac{\partial w}{\partial \theta} \right) \right] + N_{rr} \vartheta_r + N_{r\theta} \vartheta_\theta$$

The Rayleigh–Ritz method is one of the methods for solving the problem of the finite buckling of a shallow spherical dome. In order to employ this method, the displacements of the points of the middle surface of the dome are represented by the functional sums

$$\begin{aligned} u^* &= \sum_{i=1}^{K_o} U_{oi} u_{oi}(\rho) + \sum_{i=1}^{K_a} U_{ai} u_{ai}(\rho) \cos(n_i \theta) \\ v^* &= \sum_{i=1}^{K_a} V_{ai} v_{ai}(\rho) \sin(n_i \theta) \\ w^* &= \sum_{i=1}^{K_o} W_{oi} w_{oi}(\rho) + \sum_{i=1}^{K_a} W_{ai} w_{ai}(\rho) \cos(n_i \theta); \quad \rho = \frac{r}{a} \end{aligned} \quad (1.6)$$

where terms with the subscript  $o$  are the axisymmetric components of the solution, those with the subscript  $a$  are the non-axisymmetric components, the number of the non-axisymmetric harmonics  $n_i$  are specified in advance,  $U_{oi}$ ,  $U_{ai}$ ,  $V_{ai}$ ,  $W_{oi}$  and  $W_{ai}$  are the required generalized displacements and, starting from the structure of the equilibrium equations for the dome (1.4) and boundary conditions (1.5), we represent the basis functions  $u_{oi}(\rho)$ ,  $u_{ai}(\rho)$ ,  $v_{ai}(\rho)$ ,  $w_{oi}(\rho)$  and  $w_{ai}(\rho)$  in the following form

$$\begin{aligned} u_{oi}(\rho) &= A_{oi} J_1(\nu_{oi} \rho), \quad i = \overline{1, K_o} \\ w_{oi}(\rho) &= C_{oi} [J_0(\omega_{oi} \rho) - b_{oi} I_0(\omega_{oi} \rho)], \quad i = \overline{1, K_o} \\ u_{ai}(\rho) &= A_{ai} J_{n_i+1}(\nu_{ai} \rho), \quad i = \overline{1, K_a} \\ v_{ai}(\rho) &= B_{ai} J_{n_i+1}(\mu_{ai} \rho), \quad i = \overline{1, K_a} \\ w_{ai}(\rho) &= C_{ai} [J_{n_i}(\omega_{ai} \rho) - b_{ai} I_{n_i}(\omega_{ai} \rho)], \quad i = \overline{1, K_a} \end{aligned}$$

Here,  $J_{n_i}$  and  $J_{n_i+1}$  are  $n_i$ th and  $(n_i + 1)$ th order Bessel function of the first kind,  $I_{n_i}$  are modified  $n_i$ th order Bessel functions of the first kind, and the constants  $A_{oi}$ ,  $C_{oi}$ ,  $b_{oi}$ ,  $A_{ai}$ ,  $B_{ai}$ ,  $C_{ai}$  and  $b_{ai}$  and the coefficients  $\nu_{oi}$ ,  $\omega_{oi}$ ,  $\nu_{ai}$ ,  $\mu_{ai}$  and  $\omega_{ai}$  are determined from the boundary conditions.

For displacements of the dome in the form of (1.6), the potential energy of deformation of the shallow spherical dome (1.1) and the work of the external load (1.2), after integration has been carried out, is described in the form of finite sums, the arguments of which are the generalized displacements of the dome  $U_{oi}$ ,  $U_{ai}$ ,  $V_{ai}$ ,  $W_{oi}$  and  $W_{ai}$ .

The further implementation of the Rayleigh–Ritz method enables one to obtain the equilibrium equations of the shell in terms of the generalized displacements. For this purpose, the potential energy of deformation  $\Pi$  and the work of the external load  $A$  are substituted in the form of finite sums into the Lagrange equation (1.3), whereupon a system of non-linear algebraic equations is obtained which, in matrix notation, has the form

$$\mathbf{f}(\mathbf{x}) = 0 \tag{1.7}$$

For the vector  $\mathbf{f} = (F_1 F_2 \dots F_{N_{\max}})^T$ , we have in mind a vector composed of the partial derivatives of the total potential energy of deformation of the shell  $\Theta = \Pi - A$  with respect to the displacements  $U_{oi}$ ,  $W_{oi}$  ( $i = \overline{1, K_0}$ ) and  $U_{ai}$ ,  $V_{ai}$ ,  $W_{ai}$  ( $i = \overline{1, K_a}$ ). In accordance with the idea of the variables of the solution having equal rights, the vector  $\mathbf{x}$  is made up of the generalized displacements, to the number of which the dimensionless transverse load is added,

$$\mathbf{x} = (U_{o1}, W_{o1}, U_{o2}, W_{o2}, \dots, U_{oK_0}, W_{oK_0}, U_{a1}, V_{a1}, W_{a1}, U_{a2}, V_{a2}, W_{a2}, \dots, U_{aK_a}, V_{aK_a}, W_{aK_a}, q^*)^T$$

The solution of the system of non-linear algebraic equations (1.7), the order of which, for simplicity, is assumed from now on to be equal to  $n$ , is constructed by the method of continuous prolongation, which is based on the numerical solution of the Cauchy problem corresponding to it with zero initial conditions describing the unloaded state of the shell.

To do this, the system of linear algebraic equations

$$\mathbf{J}\mathbf{q} = \mathbf{b} \tag{1.8}$$

is solved far from the bifurcation points in a similar manner to that described earlier in [26] at each step with respect to the parameter  $\lambda$ , where  $\mathbf{J}$  is the extended and supplemented Jacobian of the system of non-linear algebraic equations (1.7),  $\mathbf{q}$  is the prolongation vector of the solution  $\mathbf{x}$  and  $\mathbf{b}$  is the vector of the right-hand sides of the system of prolongation equations

$$\mathbf{J} = \begin{vmatrix} F_{1,1} & \dots & F_{1,n} & F_{1,n+1} \\ \dots & \dots & \dots & \dots \\ F_{n,1} & \dots & F_{n,n} & F_{n,n+1} \\ F_{1,n+1} & \dots & F_{n,n+1} & \varepsilon \end{vmatrix}, \quad \mathbf{q} = \begin{vmatrix} \varphi_1 \\ \dots \\ \varphi_n \\ \varphi_{n+1} \end{vmatrix}, \quad \mathbf{b} = \begin{vmatrix} 0 \\ \dots \\ 0 \\ b \end{vmatrix}$$

The elements of the Jacobian  $\mathbf{J}$  are calculated as the partial derivatives of the left-hand sides of system of non-linear algebraic equations (1.7) using the arguments of the solution, among which the dimensionless load  $q^*$  is included. The parameter  $\varepsilon$  of system (1.8) is chosen from the condition of the best possible conditionality of the Jacobian of this system and the parameter  $b$  is chosen from the condition for the prolongation vector of the solution  $\mathbf{q}$  to be close to the normalized vector:  $\|\mathbf{q}\| = 1$ . As a result, the vector  $\mathbf{q}$ , which, from as a geometrical point of view, is a tangential vector to the loading trajectory, is the vector of the right-hand sides of the normal system of ordinary differential equations

$$d\mathbf{x}/d\lambda = \mathbf{q}(\mathbf{x}) \tag{1.9}$$

the numerical solution of which gives the coordinates of the points of the loading trajectory of the shell.

In order to compensate for the errors in determining the vector  $\mathbf{x}$ , which accumulate during the numerical solution of the system of prolongation equations (1.8), the method of discrete prolongation [27] is used beyond the bifurcation points. The basis of this technique is Newton’s method, which has been implemented for an extended variable space. In accordance with the approach described previously in [27], each iteration of Newton’s method is carried out by solving a system of linear algebraic equations of the form

$$\mathbf{J}\Delta\mathbf{x} = \mathbf{f}_o \tag{1.10}$$

where  $\Delta\mathbf{x}$  is the vector of the discrepancies of the solution and  $\mathbf{f}_o$  is the augmented vector of the left-hand sides of the system of non-linear algebraic equations (1.7):

$$\Delta\mathbf{x} = (\Delta x_1, \Delta x_2, \dots, \Delta x_{n+1})^T, \quad \mathbf{f}_o = (F_1, F_2, \dots, F_n, 0)^T$$

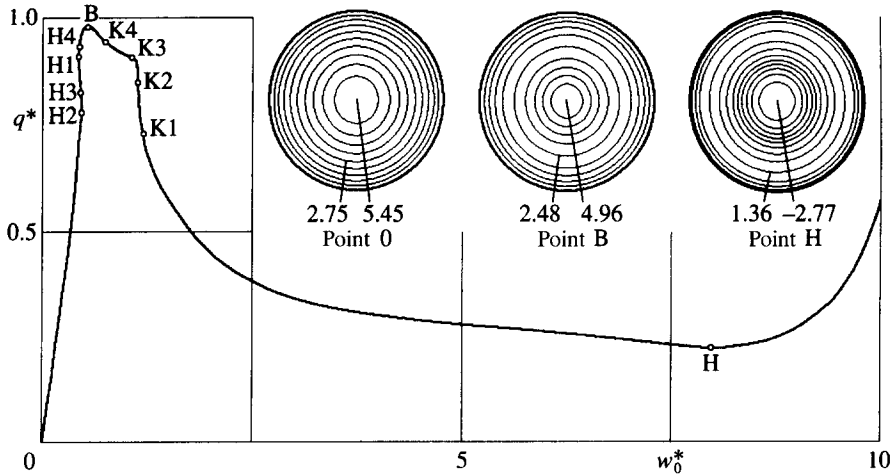


Fig. 2

The system of linear algebraic equations (1.7) is ill-posed in the neighbourhood of the bifurcation points and degenerate at a bifurcation point itself. It is impossible to calculate the prolongation vector  $\mathbf{q}$  and to obtain the solution of system of differential equations (1.9). Hence, in this situation, a modification of the prolongation method is used [28]. It consists of the fact that the prolongation vector  $\mathbf{q}$ , which is the vector of the right-hand sides of system (1.9), is sought in the neighbourhood of a bifurcation point and at the bifurcation point itself as a linear combination of the eigenvectors of the algebraic eigenvalue problem

$$\mathbf{J}\mathbf{q} = \omega\mathbf{q} \tag{1.11}$$

It has been shown [28] that the eigenvectors of this problem, which have a null  $(n + 1)$ th component, are bifurcation components and, by using them, it is possible to extend the solution from a bifurcation point along any chosen branch. The remaining eigenvectors are answerable for the formation of the prolongation vector along the main branch of the loading trajectory and the process of prolongation of the solution again reduces to solving the Cauchy problem for system of differential equations (1.9).

The refinement of the solution in the neighbourhood of bifurcation points as well as its prolongation is carried out using a special algorithm [29]. It is constructed on the solution of the eigenvalue problem (1.11). Using its eigenvectors, a discrepancy vector  $\Delta\mathbf{x}$ , which refines the solution, is constructed using the given technique at each iteration of Newton's method, depending on where the refinement is carried out: on the main branch of the loading trajectory or on the bifurcation branch.

## 2. ANALYSIS OF THE POSTBUCKLING BEHAVIOUR OF A DOME

An ideal shallow spherical dome is an axisymmetric shell. Its loading with an axisymmetric load, that is, with a uniform transverse pressure, gives rise to axisymmetric deformations in it. The axisymmetric loading trajectory of an elastic dome with a wall-thickness parameter  $\mu = 6$ , which can correspond to a dome with  $R/h = 100$ ,  $\varphi_0 = 19^\circ$  and  $\nu = 0.3$ , and a uniform transverse pressure is shown in Fig. 2. In this figure, there is a linear deformation segment and a non-linear deformation segment in which there are two limiting points: point B and point H. These points divide the axisymmetric loading trajectory into stable and unstable segments. The segments 0B and to the right of point H are the geometrical location of points corresponding to stable equilibrium states of the dome while the segment BH corresponds to its unstable equilibrium states. The initial shape of the undeformed dome (the point 0) and the shapes of the deformed surface of the dome at points B and H are shown in the right-hand upper part of Fig. 2 (henceforth, the external periphery corresponds to a zero dimensionless  $z$  coordinate of the dome  $z^* = z/h = 0$ ). At point B, the dome loses stability by snapping. The ordinate of this point determines the upper critical load. At this point, the dome has a neutral equilibrium state and, upon the infinitesimal increase in loading, transfers by snapping to a new stable state, which is described by a point located in the loading trajectory to the right of point H and having the same ordinate as point B. If the dome snapped under the action of the load and finds itself in a stable equilibrium state described by points to the right of point H, then, in proportion to the removal of the load, the point corresponding

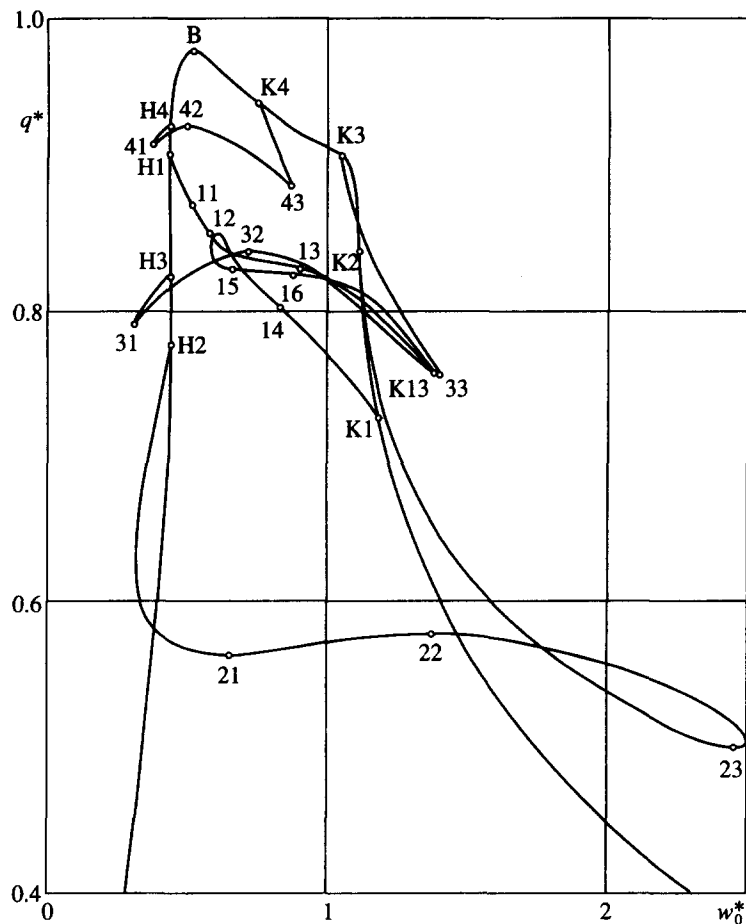


Fig. 3

to the equilibrium state of the dome will “sink” along the loading trajectory to the point H. The ordinate of this point determines the lower critical load of the dome. At this point, the dome again acquires a state of neutral equilibrium and, where there is a further reduction in the load, will click out and return to a shape which is close to the initial unloaded shape, described by a point in the segment OB of the loading trajectory with an ordinate which is equal to the ordinate of point H.

The existence of the bifurcation points H1, ... , H4, K1, ... , K4 (Fig. 2) in the loading trajectory of the dome suggests that, under the action of an axisymmetric load, it can be deformed non-axisymmetrically. At all these points, the dome has axisymmetric, neutral, equilibrium states, as a Eulerian loss of stability of the dome occurs at points H1, ... , H4 with the formation of one, two, three or four waves along the periphery, respectively. The existence of similar points K1, ... , K4 in the unstable segment of the trajectory BH suggests that, at these points, together with the unstable, axisymmetric, stress-strain state, unstable, non-axisymmetric stress-strain states with one, two, three or four waves along the circumference respectively are also characteristic of the shell.

Bifurcation branches of the loading trajectory emerge from these points. These branches are the locus of unstable, non-axisymmetric equilibrium states of the dome and are shown in Fig. 3. Each of them, with the exception of the branch which corresponds to equilibrium states with a single wave along the circumference, begins at the points H2, H3 and H4 and terminates at the points K2, K3 and K4. The bifurcation branch, which describes a stress-strain state with as a single wave along the circumference, consists of two parts, each of which begins in the axisymmetric part of the loading trajectory at the points H1 and K1 and terminates at the point K13 on the bifurcation branch joining the points H3 and K3. The forms of the deformed surface of the dome at points of the bifurcation branches of the loading trajectory are shown in Figs 4–7.

One emerging from each bifurcation point in the stable segment of the axisymmetric loading trajectory OB, non-axisymmetric deformations of the dome, which acquire an ever more noticeable character as

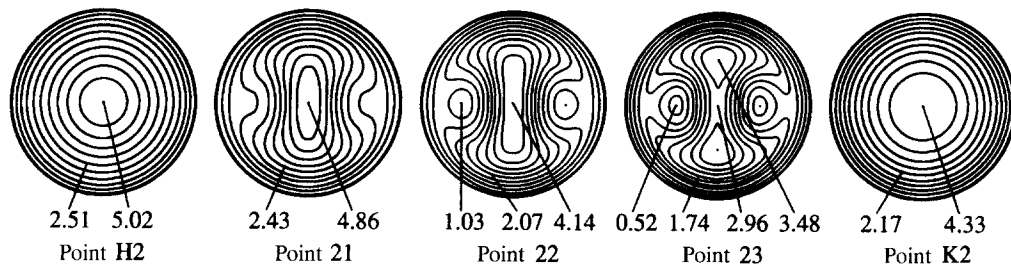


Fig. 4

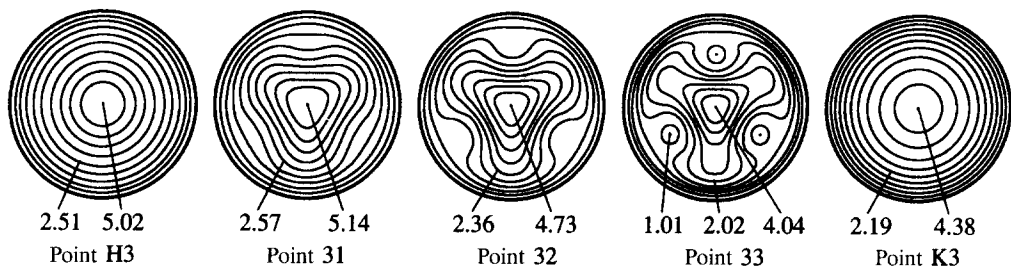


Fig. 5

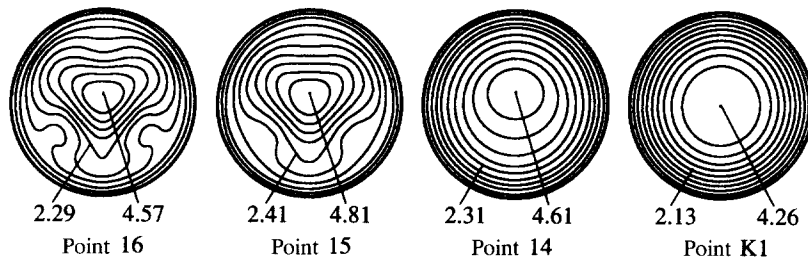
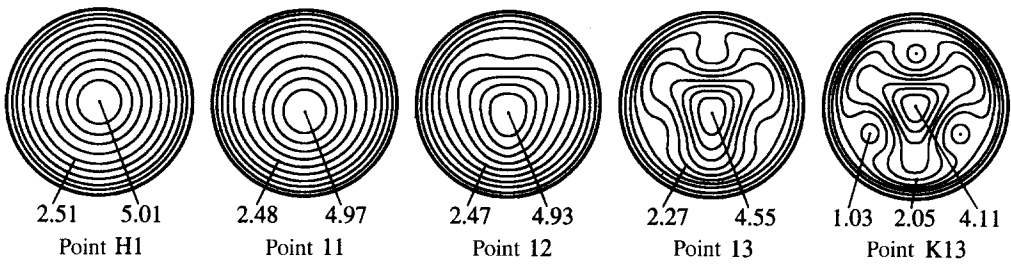


Fig. 6

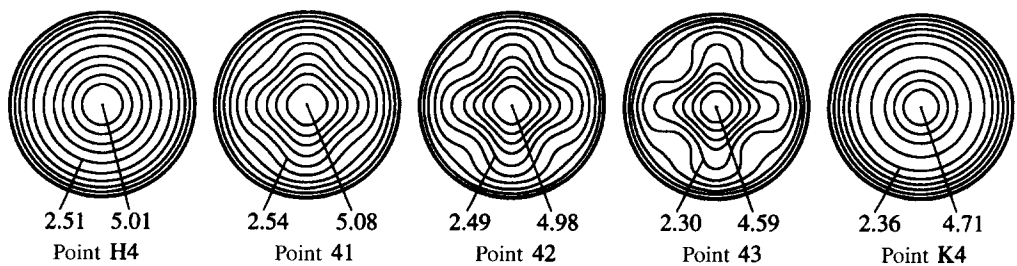


Fig. 7



the distance from the bifurcation point increases, are superimposed on the axisymmetric deformations. However, on approaching the bifurcation points in the unstable segment of the axisymmetric loading trajectory BH, the non-axisymmetric components of the deformation disappear and the dome shape becomes axisymmetric at a bifurcation point. This holds for all of the bifurcation branches apart from the branches emerging from the points H1 and K1. On emerging from these points of the dome, non-axisymmetric components with a single wave along the circumference appear. However, at deflection values at the pole of the dome of 0.6–0.7 of the thickness, components with three waves begin to be superimposed on the non-axisymmetric components with a single wave along the circumference, and the bifurcation branches, instead of joining, turn towards the unstable segment of the axisymmetric trajectory. At the same time, the non-axisymmetric components with three waves along the circumference acquire a decisive character, suppressing the non-axisymmetric components with a single wave. As a result, on approaching the bifurcation point K13, the dome has a shape which is characteristic of a branch with three waves along the circumference (Fig. 5).

The deformation pattern for the shallow spherical dome shown in Fig. 3 is only characteristic of a shell of ideal shape. Since a real spherical shell necessarily has small deviations from an ideal spherical form. Hence, when a dome is loaded with a uniform transverse load, it will, from the very beginning, be deformed in a non-axisymmetric manner depending on which component of the initial inaccuracy predominates in the case of that dome. It will lose stability by snapping, as has been shown in [22–25], where a maximum non-axisymmetric deviation in the form of a spherical shell from the ideal of no greater than 7% of its thickness and a maximum axisymmetric deviation of no greater than 20% were observed. The upper critical load for such snapping will be defined by the load values, which are characteristic in the case of the limiting points of the bifurcation branches of an ideal shell. It will be somewhat smaller than these values which, in the case of the shallow dome under consideration, lie in the range from 0.5 to 0.9 (see Fig. 3). Depending on the nature and the magnitude of the initial imperfection of the dome, its critical load must take values from a range with a lower boundary which is less than 0.5. This assumption is fully in accord with the experimental data, which are shown in Fig. 1. In particular, for a wall-thinness parameter  $\mu = 6$ , the experimentally found values of the critical loads of a shallow spherical dome lie in the range from 0.37 to 0.88.

### 3. THE ACCURACY OF THE DETERMINATION OF CRITICAL LOADS

An analysis of the chosen computational scheme and the results of an investigation of the error in the calculations enables us to assert that the solution of the problem of the geometrically non-linear deformation of a shallow, elastic spherical dome can be obtained with a relative error which does not exceeds 5%.

In fact, under conditions of the elastic deformation of a dome, the Marguerre equations for shallow shells of finite deflection are considered to be quite accurate. The sources of error in these equations arise from the assumption regarding the elasticity of the deformation of the dome, the quadratic law for representing the deformations and the assumption regarding the shallowness of the shell. However, according to existing estimates for shells with an aperture angle no greater than  $22^\circ$  and having deflections less than ten thicknesses, the error in determining such an integral characteristic of the shell as its critical load does not exceed 5%. The errors in the methods of solving the system of non-linear, algebraic, equilibrium equations (1.7), that is, the errors in the Gauss, Newton, Jacobi and Kutta–Merson methods, were monitored at each step in the calculations and, in their relative magnitude, did not exceed  $10^{-5}$ , which is considerably less than the errors in the mathematical model. The same also applies to the error in using the Rayleigh–Ritz method, which was determined numerically by calculations with different numbers of terms in the sums (1.6), which approximate the displacements. They show that, to calculate the critical loads of a dome with an accuracy of up to three significant figures, it suffices to take account of six terms of the axisymmetric solution, five terms with  $\cos\theta$ , five terms with  $\cos 2\theta$ , three terms with  $\cos 3\theta$  and three terms with  $\cos 4\theta$ .

### 4. CONCLUSION

The analysis of the non-axisymmetric, postbuckling deformation of a shallow spherical dome which has been presented enables us to suggest that the observed scatter in the experimental values for its critical loads are primarily caused by the existence of axisymmetric and non-axisymmetric initial shape imperfections in it, and is most likely determined by the form of these deviations, rather than by their magnitude. The value of the critical load must depend on which component of the initial imperfection

in the dome, of the number of forms of its postbuckling, unstable equilibrium states which have been found, predominates in the case of this dome. The introduction into the calculation of the deformation of a dome of small initial imperfections in the nature of its forms of non-axisymmetric, postbuckling equilibrium should enable the scatter in the values of the critical load observed in experiments to be modelled.

## REFERENCES

1. BACH, C., Die Widerstandfähigkeit kugelförmiger Wandungen gegenüber äusserem über Druck. *Z. Vereines deutscher Ingenieure*, 1902, **46**, 10, 333–341.
2. ZOLLY, R., *Über ein Knickungsproblem an der Kugelschale. Promotionsarbeit*. Technische Hochschule, Zurich, 1915.
3. SCHWERIN, E., Zur Stabilität der dünnwandigen Hohlkugel unter gleichmäßigem Außendruck. *ZAMM*, 1922, **2**, 2, 81–91.
4. KARMAN, Th. and TSIEN, S., The buckling of spherical shells by external pressure. *J. Aeronaut. Sci.*, 1939, **7**, 2, 43–50.
5. TIMOSHENKO, S. P. and WOINOWSKY-KRIEGER, S., *Theory of plates and shells*. McGraw-Hill, New York, 1959.
6. VOLMIR, A. S., *The Stability of Deformable Systems*. Nauka, Moscow, 1967.
7. GRIGOLYUK, E. I. and KABANOV, V. V., *The Stability of Shells*. Nauka, Moscow, 1978.
8. KARMAN, Th. and KERR, A. D., Instability of spherical shells subjected to external pressure. *Topics Appl. Mech. Amsterdam*, 1965, 1–22.
9. SUNAGAWA MEGUMI and KUMAI NORI, The resistance of structural components to dynamic loading, *J. Japan. Soc. Aeronaut. and Space Sci.*, 1970, **18**, 195, 154–166.
10. VOROVICH, I. I. and MINAKOVA, N. I., The problem of stability and numerical methods in the theory of spherical shells. In *Advances in Science and Technology. Mechanics of Deformable Solids*. VINITI, Moscow, 1973, **7**, 5–86.
11. GRIGOLYUK, E. I. and MAMAI, V. I., *The Mechanics of the Deformation of Spherical Shells*. Izd. MGU, Moscow, 1983.
12. MESCALL, J., Numerical solutions of non-linear equations for shells of revolution. *AIAA J.* 1966, **4**, 11, 2041–2043.
13. GAVRYUSHIN, S. S., Numerical modelling and analysis of the non-linear deformation of flexible shells. *Izv. Ross. Akad. Nauk. MTT*, 1994, **1**, 109–119.
14. GRIGOLYUK, E. I. and LOPANITSYN, Ye. A., Axisymmetric postbuckling behaviour of shallow spherical domes. *Prikl. Mat. Mekh.*, 2002, **66**, 4, 621–634.
15. GRIGOLYUK, E. I., The stability of a spherical shell in the case of finite deflections and asymmetric deformation. *Izv. Akad. Nauk SSSR, Otd. Tekhn. Nauk, Mekh. i Mashinostroyeniye*, 1960, **6**, 68–73.
16. GRIGOLIUK, E. I., On the unsymmetrical snapping of shell of revolution. *Proc. IUTAM Sympos. on the Theory of Thin Elastic Shells*, Delft, 1959. North-Holland, Amsterdam, 1960, 112–121.
17. WEINITSCHKE, H. J., Asymmetric buckling of clamped shallow spherical shell. *NASA Techn. Notes*, 1962, D-1510, 481–490.
18. GJELSVIK, A. and BODNER, S. R., Nonsymmetrical snap buckling of spherical caps. *J. Engng. Mech. Div.*, 1962, **88**, 5, 135–167.
19. PARMETER, R. R. and FUNG, Y. C., On the influence of nonsymmetrical modes on the buckling of shallow spherical shells under uniform pressure. *NASA Techn. Notes*, 1962, D-1510, 491–502.
20. HUANG, N.-C., Unsymmetrical buckling of thin shallow spherical shells. *AIAA J.*, 1963, **1**, 945; *Trans. ASME, Ser. E.*, 1964, **31**, 447–457.
21. GRIGOLYUK, E. I. and LIPOVTSEV, Yu. V., The local stability of elastic shells of revolution. *Mekh. Tverd. Tela. Inzh. Zh.*, 1968, **6**, 134–138.
22. YAMADA, S., UCHIYAMA, K. and YAMADA, M., Experiments on the buckling of clamped shallow spherical shells under external pressure. *Technol. Repts Tohoku Univ.*, 1980, **45**, 205–228.
23. YAMADA, S., Uchiyama, K. and YAMADA, M., Experimental investigation of the buckling of shallow spherical shells. *J. Non-Linear Mech.*, 1983, **18**, 37–54.
24. YAMADA, M. and YAMADA, S., Agreement between theory and experiment on large-deflection behaviour of clamped shallow spherical shells under external pressure. *Collapse* (Edited by J.M.T. Tompson and J.W. Hant). Cambridge University Press, Cambridge, 1983, 431–441.
25. UCHIYAMA, M. and YAMADA, S., Nonlinear buckling simulations of imperfect shell domes using a hybrid finite element formulation and the agreement with experiments. *Computation Methods. Shell and Spatial Structures* (Edited by M. Papadrakakis et al.). Athens, ISASR-NTUA. IASS-IACM. 2000.
26. GRIGOLYUK, E. I. and LOPANITSYN, Ye. A., The method of continuous prolongation with respect to a parameter, *Dokl. Ross. Akad. Nauk*, 1994, **335**, 5, 582–585.
27. GRIGOLYUK, E. I. and LOPANITSYN, Ye. A., A modification of the method of discrete prolongation with respect to a parameter. *Zh. Prikl. Mekh. Tekh. Fiz.*, 1990, **5**, 95–99.
28. GRIGOLYUK, E. I. and LOPANITSYN, Ye. A., Prolongation of the solution of non-linear equations in the neighbourhood of bifurcation points. *Matematichni Metodi ta Fiz. Mekh Polya*, 1998, **41**, 1, 35–46.
29. GRIGOLYUK, E. I. and LOPANITSYN, Ye. A., *Lifespans. On the 85th year of B. V. Raushenbach*. Nauka, Moscow, 1999, 192–199.

Translated by E.L.S.